



ACCEPTED MANUSCRIPT

Exponential horn revisited: wave equation, normal modes and experimental measurements

To cite this article before publication: Maricel Matar *et al* 2023 *Eur. J. Phys.* in press <https://doi.org/10.1088/1361-6404/acbef0>

Manuscript version: Accepted Manuscript

Accepted Manuscript is “the version of the article accepted for publication including all changes made as a result of the peer review process, and which may also include the addition to the article by IOP Publishing of a header, an article ID, a cover sheet and/or an ‘Accepted Manuscript’ watermark, but excluding any other editing, typesetting or other changes made by IOP Publishing and/or its licensors”

This Accepted Manuscript is © 2023 European Physical Society.

During the embargo period (the 12 month period from the publication of the Version of Record of this article), the Accepted Manuscript is fully protected by copyright and cannot be reused or reposted elsewhere.

As the Version of Record of this article is going to be / has been published on a subscription basis, this Accepted Manuscript is available for reuse under a CC BY-NC-ND 3.0 licence after the 12 month embargo period.

After the embargo period, everyone is permitted to use copy and redistribute this article for non-commercial purposes only, provided that they adhere to all the terms of the licence <https://creativecommons.org/licenses/by-nc-nd/3.0>

Although reasonable endeavours have been taken to obtain all necessary permissions from third parties to include their copyrighted content within this article, their full citation and copyright line may not be present in this Accepted Manuscript version. Before using any content from this article, please refer to the Version of Record on IOPscience once published for full citation and copyright details, as permissions will likely be required. All third party content is fully copyright protected, unless specifically stated otherwise in the figure caption in the Version of Record.

View the [article online](#) for updates and enhancements.

Exponential horn revisited: wave equation, normal modes and experimental measurements

M. Matar¹, M.A. Parodi¹, L. Raviola¹, I. Novara^{1,2}, F. Vera¹,
B.J. Gómez^{1,2}, A. Roatta^{1,2}, C.E. Repetto^{1,2}

¹ Facultad de Ciencias Exactas, Ingeniería y Agrimensura (UNR), Av. Pellegrini 250, S2000BTP Rosario, Argentina.

² Instituto de Física Rosario (CONICET-UNR), Bv. 27 de Febrero 210 Bis, S2000EYP Rosario, Argentina.

E-mail: repetto@ifir-conicet.gov.ar

Abstract. In this work, a theoretical analysis is first presented to find the wave equation corresponding to the propagation of disturbances in the air contained inside a tube of variable cross section. In particular, the case of a tube with a circular cross section whose area varies exponentially as a function of the axial coordinate is studied. The hypotheses of the model used are discussed and the solutions of the wave equation obtained are presented. Secondly, and with the aim of validating the model used, measurements are made on a tube such as the one described, built using a 3D printer.

Keywords: Exponential Horn, Wave Equation, Normal Modes, Impedance.

1. Introduction

The study of resonance in air columns is a standard topic in introductory physics course programs where, in general, experiments are described and performed in cylindrical tubes of constant cross section containing air at atmospheric pressure [1]. The motion of air molecules is modeled within the framework of the continuum hypothesis, meaning that every volume element is large enough to contain millions of molecules and small enough for the acoustic variables to be uniform throughout the element [2]. Pressure perturbations (waves of compression and expansion) correspond to typical changes in gas motion in the direction of propagation. In this context, the simplest mode of propagation is the plane wave. This elementary case allows for a straightforward one-dimensional treatment, approachable with the basic mathematical tools of junior undergraduate students of physics. However, the problem of wave propagation in tubes with variable cross section is rarely mentioned in the usual textbooks. From a historical perspective, this can be understood as a consequence of the higher mathematical and experimental complexities involved in the study of such systems. For reasons to be developed below, we think it is didactically useful to introduce the subject at this level of teaching. First,

by contrasting the traditional textbook approach for constant-section tubes with the more general results of the variable-section ones, we can distinguish the specific from the general aspects in the description of tubular acoustical systems. Second, an important fact to note is that for some particular but interesting geometries, problems within this class admit analytical solutions which can be readily contrasted with experimental data. In fact, it is currently feasible to build experimental devices with the desired properties using digital fabrication techniques like 3D printing, allowing the frequency spectrum of the system to be measured and analyzed in an accessible way using typical teaching laboratory facilities and resources [3]. Finally, the system can be related to common wind musical instruments, a topic with intrinsic interest that can act as a motivation.

In the present work, we investigate the resonance frequencies and oscillation modes of an air volume within a *horn* with cylindrical symmetry and exponentially growing cross sectional area, a system which satisfies the aforementioned characteristics.

In mathematical terms, a horn can be defined as any surface in which any plane perpendicular to a given line, in this case the x -axis, intersects that surface in a single closed curve C , whose interior we denote by S [4]. In the basic theory of sound propagation in horns, as in most studies done on these subjects, propagation is mainly assumed to be in the form of plane waves. This is the approach we will use in this paper, with the understanding that this is a simplification valid only for low frequencies. The derivation of the propagation equation under the assumptions of infinitesimal amplitudes and one-dimensional plane waves leads to the so-called Webster equation [5]. Usually the Webster equation is obtained from the continuity equation, which expresses the conservation of the fluid mass per unit length inside the tube, and the momentum equation, introducing the concept of potential velocity. However, in this work we will derive this equation in a more elementary way by following the guidelines of classical undergraduate textbooks for the problem of tubes of constant cross section ([6],[7],[8]). In our derivation, a careful analysis of the components of the reaction force of the tube walls will be made, procedure that has not been described in detail in previous literature, as far as we know. This sheds light on the effect of the section change on the balance of the interactions and leads to a better understanding of the phenomenon described.

The study of wave equation solutions for horns of various shapes has been analyzed by many authors. In particular, Campos [5] gives an exhaustive description of the problem and its many approaches, detailing the analytical development and applying it to different shapes of horns, for which solutions and cutoff frequencies are found. Different models for the description of the horn ending (free, flanged, unflanged) lead to different expressions for the mouth and throat impedances. The specific kind of boundary condition leads to a particular set of values for the system normal modes frequencies. The aim of the present study is to measure these frequencies in an exponential horn and to compare them with the predictions of various theoretical models. We also show that our method allows to recover the expected results for tubes

in the limit of constant cross section.

2. Derivation of the wave equation in a variable cross section tube

Consider air as a non-viscous fluid in contact with the pipe walls, which are considered perfectly smooth. We will describe the behavior of the fluid macroscopically, within the framework of the continuum model. We divide the cylinder into N identical slices of thickness dx , as shown in Figure (1). The displacement of the fluid is the displacement of the centre of mass of these volume elements, and the pressure and density refer to the value taken by these variables in each one of these “little cylinders”. We will call ρ the density and p the pressure. Both will be functions of x and t only. This is a simplification of the description of the system that allows it to be considered one-dimensional, i.e. the whole section of equal x coordinate moves under the action of the same forces.

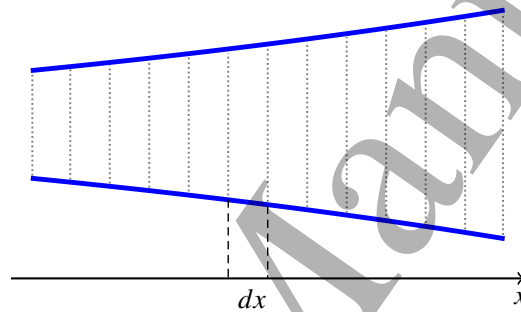


Figure 1. Division of the tube of variable section in “little cylinders” of length dx .

We will always consider an infinitesimal volume element which is small from the macroscopic point of view but large compared to the distances between molecules. When we speak of its displacement, we mean the displacement of that volume element containing a large number of molecules.

Implicit in the continuum model is the assumption that two neighbouring points have very similar motions. This hypothesis allows us to describe the vector displacement of all particles in a small environment around the point x, y, z by means of a continuous vector field $\Phi(x, y, z, t)$. It is important to note that the x, y, z are the coordinates of the equilibrium position of the particles. If the wave is a scalar, the perturbation is a continuous scalar function of the position. For example, the pressure of an acoustic wave $p = p(x, y, z, t)$, from the mathematical point of view, is a continuous time-varying scalar field.

Let us first analyze the change that occurs in a volume element inside the tube when it is perturbed by the wave passing through it. This is depicted schematically in Figure 2. We assume that before the wave passes through, the air is at an equilibrium pressure p_0 and has a volume density ρ_0 . Therefore, in the equilibrium state, the volume

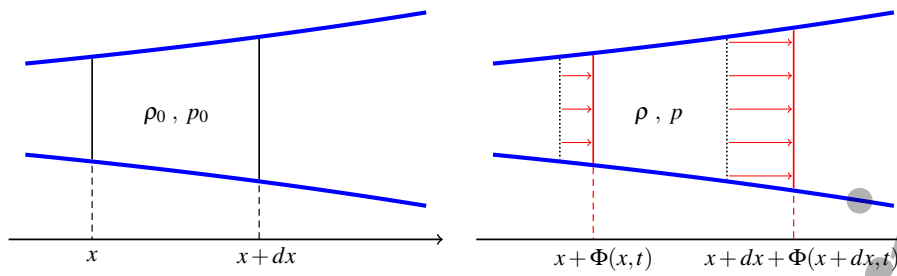


Figure 2. Representation of a volume element when perturbed by the wave $\Phi(x, t)$.

of that element is $V_0 = S(x)dx$ (itself another approximation) and the mass of air will be $\rho_0 V_0$ (see Figure 2, left-hand side).

When the wave reaches that volume element, its boundary surfaces move (see Figure 2, right-hand side) and the perturbed volume is given by the expression

$$\begin{aligned} V &= S(x + \Phi(x, t)) \cdot [x + dx + \Phi(x + dx, t) - (x + \Phi(x, t))] \\ &= \left(S(x) + \frac{dS(x)}{dx} \Phi(x, t) \right) \left(dx + \frac{\partial \Phi(x, t)}{\partial x} dx \right). \end{aligned} \quad (1)$$

Disregarding higher-order terms, we obtain the change in volume as

$$\Delta V = V - V_0 \approx \frac{\partial}{\partial x} (S(x)\Phi(x, t)) dx. \quad (2)$$

Multiplying and dividing by the section $S(x)$, the relative change in volume results in

$$\frac{\Delta V}{V_0} = \frac{1}{S(x)} \frac{\partial}{\partial x} (S(x)\Phi(x, t)). \quad (3)$$

We define the sound or acoustic pressure $p_e(x, t)$ as the first order deviations of the air pressure with respect to the equilibrium value, $p(x, t) = p_0 + p_e(x, t)$, being $|p_e(x, t)|$ (at least) four or five orders of magnitude smaller than p_0 . Then, we can relate the acoustic pressure to the relative variation of the volume given in equation (3) through the following expression:

$$p_e(x, t) = -B \frac{\Delta V}{V_0} = -\frac{B}{S(x)} \frac{\partial}{\partial x} (S(x)\Phi(x, t)), \quad (4)$$

where B is the adiabatic bulk modulus. In the case of constant cross section, we recover the usual textbook relation $p_e = -B \partial \Phi / \partial x$.

2.1. Equilibrium state

It is important to note that, even in equilibrium state, the forces acting on the cross sections bounding a given volume element are not balanced due to the change in the cross section (see Figure 3). And therefore, this volume element would acquire an acceleration. But this is not observed, due to the presence of a force that maintains the

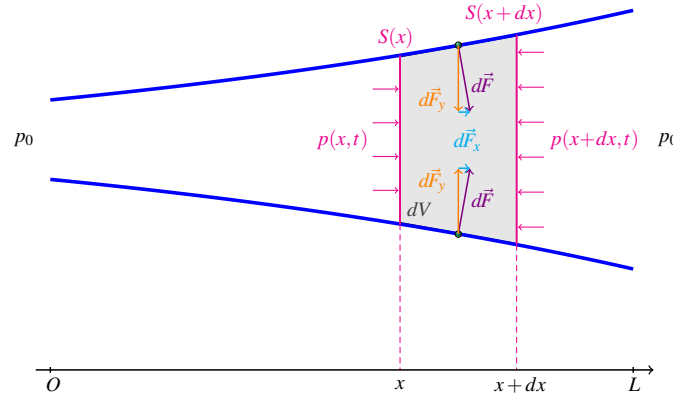


Figure 3. Forces on a volume element due to existing pressures and wall reaction.

equilibrium: this force comes from the reaction that each point of the wall of the tube exerts in its normal direction on the volume element considered. As a consequence of axial symmetry, the resultant force acts in the direction of this axis.

Therefore, in the equilibrium state, for any infinitesimal volume element inside the tube, the instantaneous acceleration of the centre of mass is the null vector. Hence, the scalar equation takes the form

$$\sum F_{ext} = p_0 S(x) - p_0 S(x + dx) + dF_x^0 = 0, \quad (5)$$

and therefore

$$dF_x^0 = p_0 (S(x + dx) - S(x)) = p_0 \frac{dS}{dx} dx. \quad (6)$$

Thus, equation (6) represents the force describing the interaction between the tube wall and the air inside the tube, which is not usually considered in detail in the literature.

In Appendix A we include a detailed calculation of this interaction for the case of a finite exponential horn.

2.2. Analysis of non-equilibrium state

We will now analyze the out-of-equilibrium situation, where the pressure $p(x, t) = p_0 + p_e(x, t)$. Analogous to the equilibrium situation, now instead of equation (6), the x -component of the wall reaction will be

$$dF_x = p(x, t) \frac{dS}{dx} dx. \quad (7)$$

Then, taking into account that the mass of the volume element under consideration is $dm = \rho_0 V_0 = \rho_0 S(x) dx$, the equation of motion now takes the form:

$$\begin{aligned} \sum F_x &= p(x, t) S(x) - p(x + dx, t) S(x + dx) + p(x, t) \frac{dS(x)}{dx} dx \\ &= -\frac{\partial (p(x, t) S(x))}{\partial x} dx + p(x, t) \frac{dS(x)}{dx} dx \end{aligned}$$

$$= -\frac{\partial p_e(x, t)}{\partial x} S(x) dx = \rho_0 S(x) dx \frac{\partial^2 \Phi(x, t)}{\partial t^2}. \quad (8)$$

Dividing by $S(x) dx$, we become independent from the volume element

$$-\frac{\partial p_e(x, t)}{\partial x} = \rho_0 \frac{\partial^2 \Phi(x, t)}{\partial t^2}. \quad (9)$$

And expressed as a function of the displacements, we use equation (4):

$$\frac{\partial}{\partial x} \left[\frac{1}{S(x)} \frac{\partial}{\partial x} (S(x) \Phi(x, t)) \right] = \frac{1}{c^2} \frac{\partial^2 \Phi}{\partial t^2}(x, t), \quad (10)$$

where $c = \sqrt{B/\rho_0}$ is the speed of sound. The latter expression is the equation for waves in tubes of variable cross section. In the case of a constant cross section, $S \neq S(x)$, the classical wave equation is recovered.

$$\frac{\partial^2 \Phi}{\partial x^2} = \frac{1}{c^2} \frac{\partial^2 \Phi}{\partial t^2}, \quad \Phi = \Phi(x, t). \quad (11)$$

3. Exponential horn

We will study a particular case of a variable cross section tube: the exponential horn. It has a circular cross section whose area varies exponentially as a function of the axial coordinate. Each cross section of the tube is located with the x coordinate, corresponding to a given point on the chosen longitudinal axis. The section $S(x = 0) = S_t$ is called the throat, while the section $S(x = L) = S_m$ is called the mouth of the horn. According to the chosen coordinate system, the area $S(x)$ of the circular section of the tube grows exponentially with the x coordinate according to the following expression:

$$S(x) = S_t e^{ax}. \quad (12)$$

Then, we have

$$a = \frac{1}{S(x)} \frac{\partial S(x)}{\partial x}. \quad (13)$$

The equation of motion (10), then, takes the form

$$\frac{\partial^2 \Phi}{\partial x^2}(x, t) + a \frac{\partial \Phi}{\partial x}(x, t) = \frac{1}{c^2} \frac{\partial^2 \Phi}{\partial t^2}(x, t), \quad (14)$$

and the relationship (4) between the acoustic pressure and the displacements results in

$$p_e(x, t) = -B \left(a + \frac{\partial}{\partial x} \right) \Phi(x, t). \quad (15)$$

The effect of the variable cross section appears as an additional term $-Ba\Phi$. Considering a harmonic solution of the form $\Phi(x, t) = \psi(x) \cdot e^{i\omega t}$ and substituting it in equation (14) results

$$\frac{d^2 \psi(x)}{dx^2} + a \frac{d\psi(x)}{dx} + k^2 \psi(x) = 0, \quad (16)$$

where ω is the angular frequency and $k = \omega/c$ is the wave number.

Stressing the formal analogy of equation (16) with the equation of motion for a damped harmonic oscillator, we propose the following solution in the spatial variable x

$$\psi(x) = e^{-\frac{a}{2}x} \cdot (C_1 e^{i\beta x} + C_2 e^{-i\beta x}), \quad (17)$$

where

$$\beta = \sqrt{k^2 - a^2/4}. \quad (18)$$

In general, for any value of ω , the solution of the wave equation is

$$\Phi(x, t) = e^{-\frac{a}{2}x} (C_1 e^{i\beta x} + C_2 e^{-i\beta x}) e^{i\omega t}, \quad (19)$$

therefore, using equation (15),

$$p_e(x, t) = -B \left[\left(\frac{a}{2} + i\beta \right) C_1 e^{-\left(\frac{a}{2} - i\beta\right)x} + \left(\frac{a}{2} - i\beta \right) C_2 e^{-\left(\frac{a}{2} + i\beta\right)x} \right] e^{i\omega t}. \quad (20)$$

In particular, in order for a wave to propagate, the following must be met

$$k^2 - \frac{a^2}{4} > 0 \Rightarrow \left(\frac{\omega}{c} \right)^2 > \frac{a^2}{4} \Rightarrow \omega > \frac{ac}{2}. \quad (21)$$

The value $\omega_c = c(a/2)$, thus constitutes a cut-off frequency and therefore propagating waves with frequencies lower than this value will not be observed.

4. Impedance and normal modes

To find and analyze the normal modes of the horn, we must consider that it has limited dimensions and we must impose boundary conditions at the ends, appropriate to what is to be investigated; that is, in order to compare the results of the different theoretical models with the values obtained from experimental measurements.

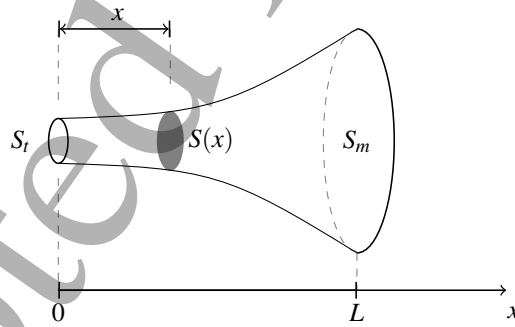


Figure 4. Scheme of the studied system. The area $S(x)$ of the circular section increases exponentially with the x coordinate.

A schematic of the system studied is shown in Figure 4. The horn has length L .

In this section we will use the concept of *acoustic impedance*. Defining the volume flow as $U = Sv$, where $v = \partial\Phi/\partial t$ is the velocity of the volume elements, and considering $p_e(x, t) = \tilde{p}(x)e^{i\omega t}$, the acoustic impedance is written as follows

$$Z(x) = \frac{p_e}{U} = \frac{\tilde{p}(x)}{S(x)i\omega\psi(x)}. \quad (22)$$

Impedances in the mouth and throat are related.

Then, using eqs. (17) and (20), we can calculate (22) at $x = 0$. Thus, the impedance at the throat results as follows

$$Z_t = Z(0) = \frac{i\rho_0 c^2}{S_t \omega} \frac{\left(\frac{a}{2} + i\beta\right) C_1 + \left(\frac{a}{2} - i\beta\right) C_2}{C_1 + C_2}. \quad (23)$$

In the same way but now for $x = L$, we have that the impedance at the mouth is

$$Z_m = Z(L) = \frac{i\rho_0 c^2}{S_m \omega} \frac{\left(\frac{a}{2} + i\beta\right) C_1 e^{i\beta L} + \left(\frac{a}{2} - i\beta\right) C_2 e^{-i\beta L}}{C_1 e^{i\beta L} + C_2 e^{-i\beta L}}, \quad (24)$$

Working with these expressions, we can write the impedance at the throat Z_t as a function of the impedance at the mouth Z_m as

$$Z_t = \left(\frac{\rho_0 c}{S_t}\right) \frac{Z_m S_m (\beta \cos \beta L - (a/2) \sin \beta L) + ik\rho_0 c \sin \beta L}{\rho_0 c (\beta \cos \beta L + (a/2) \sin \beta L) + ikZ_m S_m \sin \beta L}. \quad (25)$$

4.1. Open ends

If both the mouth and throat behave as open ends, we can search for normal modes by imposing different values to the impedances at the ends, what from now on we will call boundary conditions.

4.1.1. Zero impedances at both ends. The simplest case results from imposing zero impedances at both ends. This accounts for an ideal situation, where at the open ends the pressure is atmospheric and therefore the sound pressure is cancelled. Then, imposing $Z_t = 0$ in (23), results

$$C_2 = -\frac{(a/2 + i\beta)}{(a/2 - i\beta)} C_1. \quad (26)$$

Moreover, if we make $Z_m = 0$ in (25), we get

$$Z_t = \frac{\rho_0 c}{S_t} \frac{ik \sin(\beta L)}{(\beta \cos \beta L + (a/2) \sin \beta L)}. \quad (27)$$

and for $Z_t = 0$ to be satisfied, it must be verified that

$$\sin(\beta L) = 0 \quad \Rightarrow \quad \beta_n = n\pi/L, \quad n \in \mathbb{N}.$$

From the expression (18) the following values can be obtained for the eigenfrequencies

$$f_n = \frac{c}{2\pi} \sqrt{\left(\frac{n\pi}{L}\right)^2 + \frac{a^2}{4}}. \quad (28)$$

Therefore, we can plot the displacement and acoustic pressure wave functions, which show the behavior of the air inside the tube for the different normal modes.

For the first two normal modes, we plot in Figure 5 the envelopes of displacement and acoustic pressure as a function of the x coordinate (solid orange line). As can be seen in the graphs of Φ vs. x , both at the throat and at the mouth, the slope is not zero, as in the case of tubes of constant cross section under these boundary conditions, because

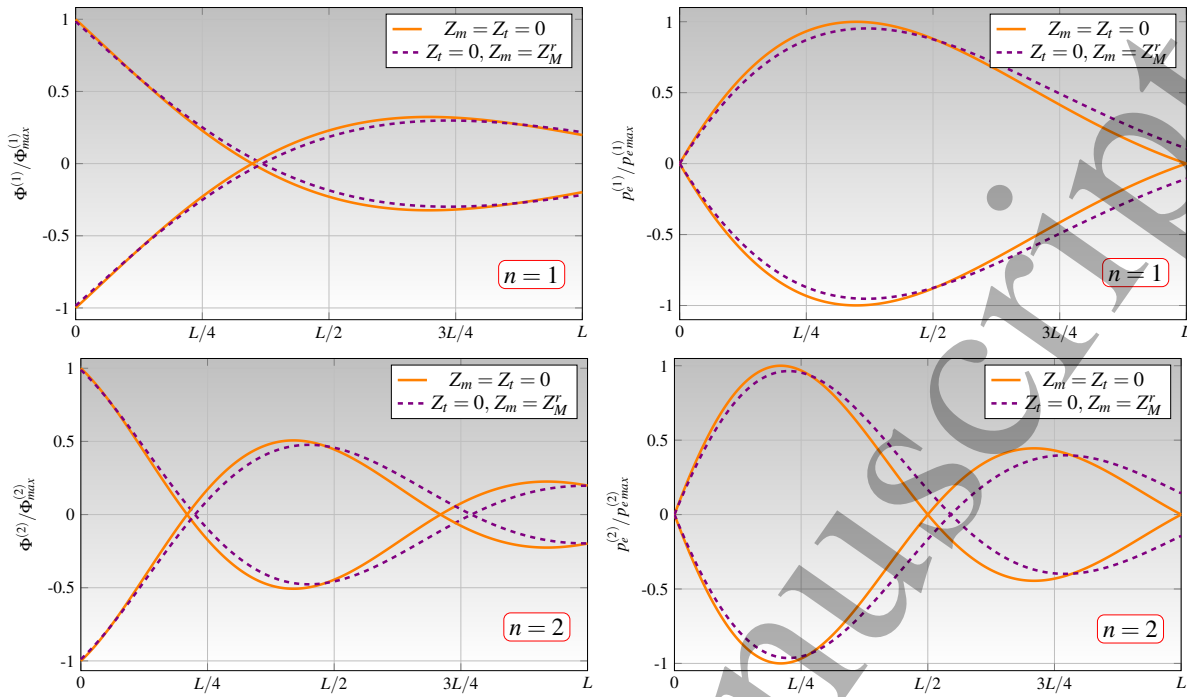


Figure 5. Envelopes of the functions (left) Φ vs. x and (right) p_e vs. x , for different boundary conditions considered. Above in the fundamental mode and below when oscillating in the second mode.

now the acoustic pressure is not directly proportional to the deformations of the volume elements because an additional term appears $a\Phi$ (see equation (15)). Furthermore, in the regions where $\partial\Phi/\partial x = 0$ it is not verified that p_e vanishes. However, as in the case of a constant cross section tube, an antinode of sound pressure coincides with a node of displacement.

When comparing the plots for the different boundary conditions in Figure (5), we can observe a shift of the nodes towards the mouth when we consider that it radiates, which is linked to a decrease in the eigenfrequencies.

4.1.2. Radiation impedance at the mouth When the system is in resonance in one of its normal modes, the mouth will be radiating energy with the highest efficiency, a fact that is seldom mentioned in undergraduate physics textbooks. In order to compare with the experimental values, we must use in the theoretical calculations expressions for radiation impedance that take into account the environment surrounding the circular aperture. We use two expressions for the mouth impedance. The first one (Z_m^r) considers a circular opening in an infinite baffle, is computationally simpler and is usually found in acoustics textbooks [10]. The second one (Z_M^r) corresponds to a disk in free space [11], is slightly involved but is more representative of our experimental setup, so we expect it will give better agreement with our measurements (see section 5). Details for both expressions

can be found in Appendix B.

From imposing $Z_m = Z_M^r$, using equation (25) Z_t can be calculated. To find the eigenfrequencies (values of f that cancel Z_t), we plot $1/|Z_t|$ and determine the values of f where the graph has peaks, as we can see in the left plot of Figure 6.

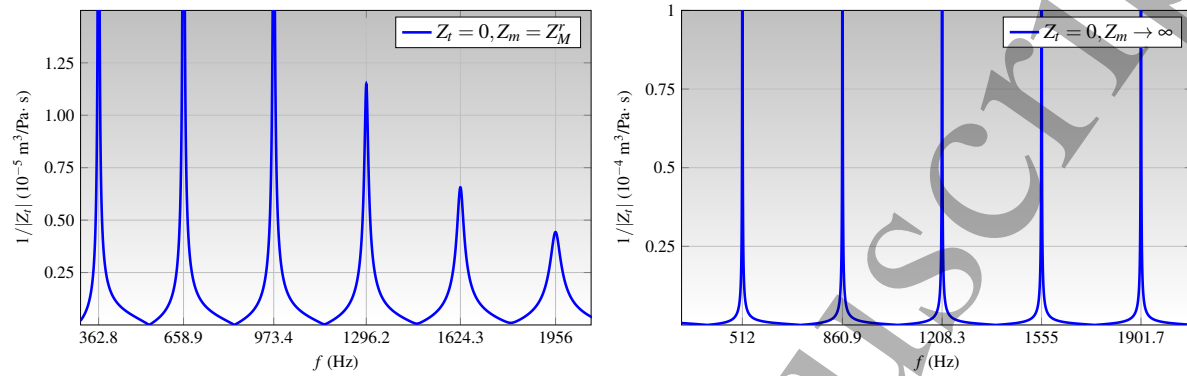


Figure 6. Eigenfrequencies considering the boundary conditions $Z_t = 0$ and (left) $Z_m = Z_M^r$ (right) $Z_m \rightarrow \infty$. The numerical values correspond to the designed exponential horn (see Section 5).

To obtain the eigenfunctions, as $Z_t = 0$, the relation between the C_1 and C_2 constants is given by the equation (26). The first two resulting modes are included in Figure 5 with a violet dashed line.

4.2. Closed mouth

If we now close the tube at the mouth but we keep the throat open, we will have to consider that $Z_m \rightarrow \infty$. Consequently,

$$Z_t = -i \frac{\rho_0 c}{k S_t} (\beta \cot \beta L - (a/2)) . \quad (29)$$

The right-hand side of Figure 6 shows the graph of $1/|Z_t|$.

The values of the abscissae correspond to the normal frequencies that verify the condition $Z_t = 0$.

When plotting the normal modes, it should be taken into account that the relation between C_1 and C_2 depends on the value of Z_t : when $Z_t = 0$ these constants are related through equation (26).

The plots of the first two normal modes are shown in Figure 7, both for Φ and for p_e .

5. Experimental setup and results discussion

The photo in Figure 8 shows the devices used to carry out the experiment. From left to right, oscilloscope, waveform generator, signal amplifier, speaker and exponential horn. We constructed the horn with a 3D printer using PLA. As can be seen in the photo,

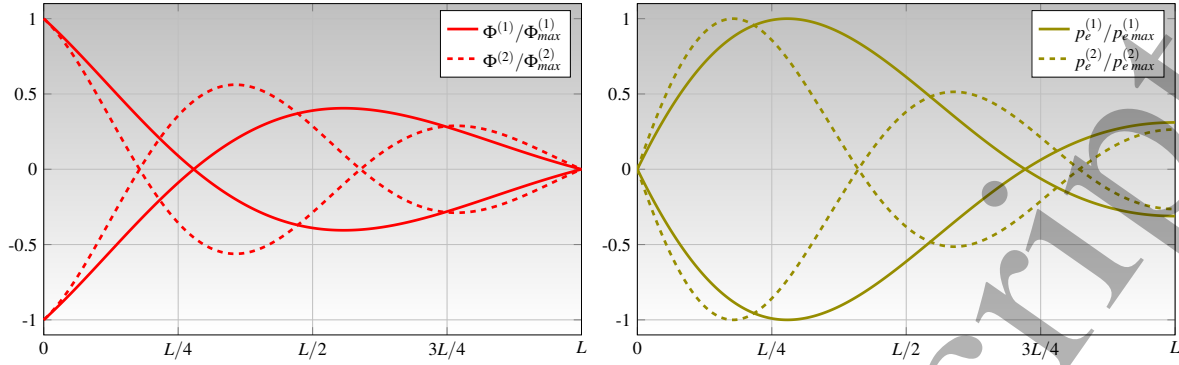


Figure 7. Envelopes of the functions (left) Φ vs. x and (right) p_e vs. x , for the closed mouth case, considering $Z_t = 0$, in the first (solid lines) and second (dashed lines) modes.

the device lies in a horizontal position and the speaker, located at a distance of 0.01 m from the throat, was controlled by a signal generator. The horn was constructed with a total length (L) of 0.5 m. The area of the circular cross section increases exponentially along its axial axis, from radius $r_0 = 0.01$ m at the throat to $r_L = 0.05$ m at the mouth. According to equation (12)

$$a = \frac{\ln(S_m/S_t)}{L} = 4 \ln(5) \text{ m}^{-1} \approx 6.44 \text{ m}^{-1}. \quad (30)$$

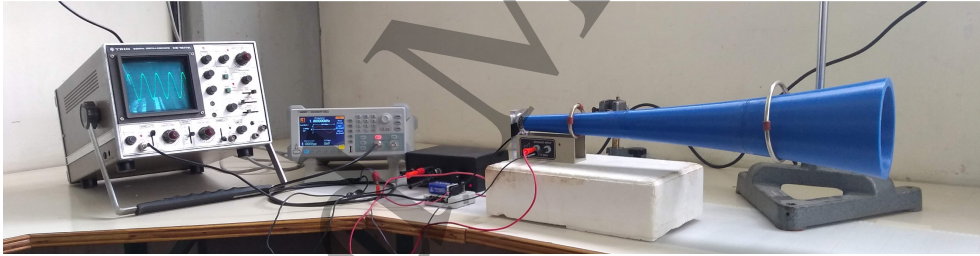


Figure 8. Arrangement of the exponential horn and other experimental devices.

On the other hand, from (21) we have that the cut-off frequency is

$$f_c = \frac{\omega_c}{2\pi} = \frac{ac}{4\pi} \approx 175.7 \text{ Hz}, \quad (31)$$

where the propagation velocity was estimated from the expression $c = \sqrt{\gamma RT/M}$ using the ambient temperature measurement.

In order to obtain the eigenfrequencies of the exponential horn in a unique record, the loudspeaker was excited by white noise. The sound signal emitted by the horn was recorded with the Ultra Linear Measurement Condenser Microphone (Behringer ECM8000) placed in the vicinity of the mouth. These sound recordings are processed by means of the Fast Fourier Transform (**FFT**) and the obtained results are then compared with the theoretical ones and are shown in Figures 9 and 10.

There is an excellent agreement between experimental and theoretical values.

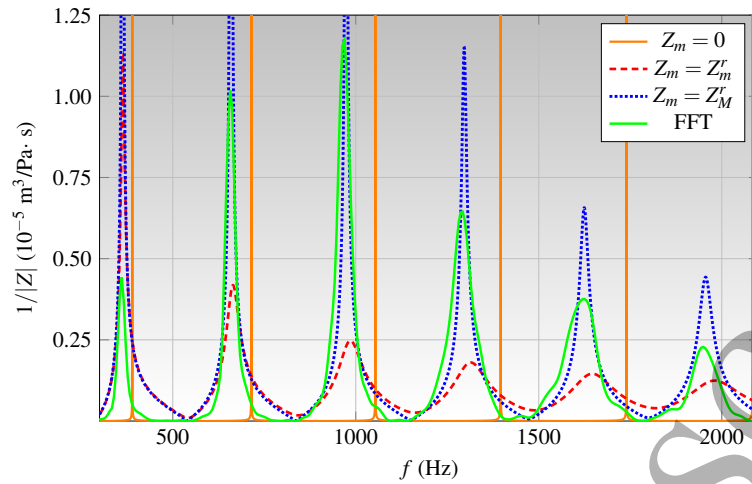


Figure 9. Results of the exponential horn with both ends open when excited with white noise. The green solid line is the **FFT** of the sound recorded by a microphone. The other curves are theoretical ones, corresponding to different boundary conditions (for the impedance) at the mouth. In all cases, $Z_t = 0$ is considered.

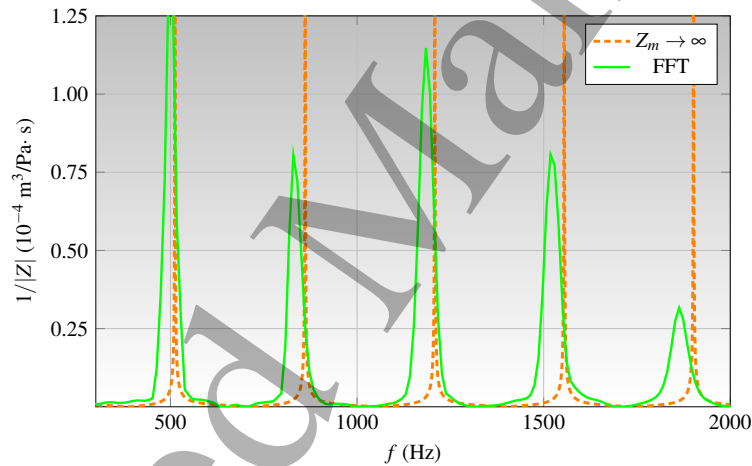


Figure 10. Results of the exponential horn closed at the mouth when excited with white noise. The green solid line is the **FFT** of the sound registered by a microphone. The dashed orange line depicts a theoretical curve, corresponding to the boundary conditions $Z_t = 0$ and $Z_m \rightarrow \infty$.

- The theoretical peaks are slightly shifted towards greater frequencies than the experimental ones obtained by means of **FFT**.
- This difference increases at higher frequencies, but the relative difference remains almost constant.
- In the case of the open mouth, these results can be seen in Figure 11. Imposing zero impedances at both ends the relative differences are between 5 and 9%. But if it is taken into account that the mouth is radiating energy, the relative differences

drop below 1.7% for the case of $Z_m = Z_m^r$, and under 0.6% for $Z_m = Z_M^r$.

- In the case of the closed mouth, considering $Z_M \rightarrow \infty$, the relative differences do not exceed 2%.
- If we took into account the uncertainty in processing experimental data with the **FFT** by choosing different windows and window sizes, those differences would have been covered.

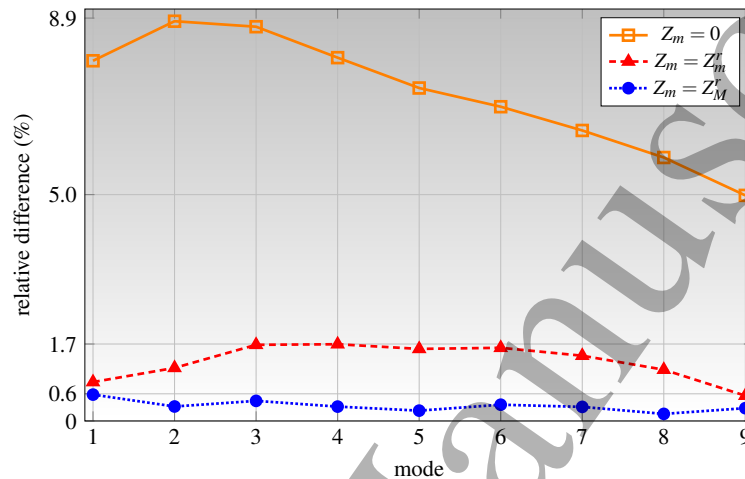


Figure 11. Relative differences between the measured values and the theoretical ones obtained for various boundary conditions at the open mouth.

6. Conclusions

In summary, we studied theoretically and experimentally the problem of acoustic waves propagating inside a horn. With this aim, we obtained the wave equation for the air contained in a tube with variable cross section. We also derived in detail the expression of the reaction force exerted by the tube walls on the air, whose interaction is not usually considered in the literature. We showed that the classical wave equation found in textbooks is recovered from our expression in the limit of constant cross section. We then solved the wave equation for the specific case of a tube with exponentially growing cross section, finding exact solutions. By considering time-harmonic solutions, we arrived to the important result that acoustic waves must have frequencies above a cut-off frequency in order to propagate inside the exponential horn. Finally, we studied the standing wave solutions (normal modes) that arise when imposing boundary conditions. These conditions were given in terms of the acoustic impedance at the ends of the horn, an original approach that we consider enlightening and complementary to those found in standard textbooks. Various boundary conditions were addressed, including the “ideal” open-open and open-close conditions at the ends of the horn, and two more

realistic models with a radiating mouth. In all cases we were able to calculate the eigenfrequencies and normal modes, stressing the differences with respect to the known results for constant cross section tubes.

In order to validate the theoretical results, we built a horn with the desired geometrical properties using 3D printing technology and compared the results with experimental measurements obtained by exciting the horn throat with white noise and recording the response with a condenser microphone. By Fourier transforming the recorded audio signal, we identified the system resonant frequencies. We found moderate agreement between the experimental values and the theoretical results for the case of both ends open (zero impedance), with relative differences in eigenfrequencies between 5 and 9% for the first 9 modes. However, the agreement improves noticeably when the radiation condition is taken into account, with the relative differences dropping below 1.7% for the case of $Z_m = Z_m^r$, and under 0.6% for $Z_m = Z_M^r$. This indicates that radiation cannot be underestimated, but this aspect is barely mentioned (if treated at all) in traditional textbooks. Finally, the fact that the theoretical frequencies always overestimate, albeit slightly, the experimental ones, could be explained from energy losses not taken into account, such as through the walls or the throat.

Appendix A. Calculation of the force exerted by the sidewall on the air inside the exponential horn

In the particular case of the horn we have constructed, the $S(x)$ area of the circular section of the tube grows exponentially with the x coordinate according to the following relation:

$$S(x) = S_0 e^{ax} = \pi r^2(x), \quad (\text{A.1})$$

where $S_0 = S(x=0) = \pi r_0^2$, and $r(x)$ is the radius of the exponentially growing horn in the x coordinate, measured from the axial axis. Then

$$r(x) = r_0 e^{\frac{ax}{2}}. \quad (\text{A.2})$$

Consequently, $r'(x)$, the derivative of r with respect to x evaluated in the x coordinate, gives us the tangent of the angle θ formed by the sidewall of the horn with the x -axis, as shown in Figure A1:

$$r'(x) = \frac{a}{2} r_0 e^{\frac{ax}{2}} = \tan \theta(x). \quad (\text{A.3})$$

Then

$$dF_x = p_0 dS \sin \theta(x) = p_0 2\pi r(x) dl \sin \theta(x) = p_0 2\pi r(x) dx \tan \theta(x) \quad (\text{A.4})$$

taking into account that $dx = dl \cos \theta(x)$, and dl is the thickness of the ring of the lateral surface dS . Integrating over the whole length of the tube, we have

$$F_x = \int_0^L dF_x = \int_0^L p_0 2\pi r_0 e^{\frac{ax}{2}} \frac{a}{2} r_0 e^{\frac{ax}{2}} dx$$

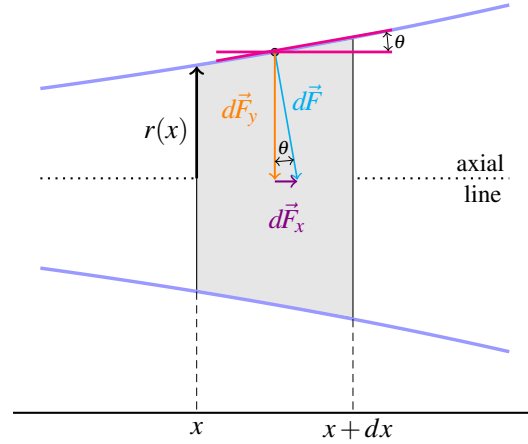


Figure A1. Reaction force of the wall pushing on the air inside the exponential horn.

$$= p_0 \pi r_0^2 a \int_0^L e^{ax} dx = p_0 (S_L - S_0) \quad (\text{A.5})$$

where $S_L = S(x = L) = \pi r_0^2 e^{aL} = \pi r_L^2$.

Appendix B. Different radiation impedance models

We work with two different expressions for the radiation impedance.

- The first expression corresponds to that of a circular opening in an infinite baffle [10]

$$Z_m = Z_m^r = \left(\frac{\rho_0 c}{S_m} \right) \left(1 - \frac{J_1(2kr_L)}{kr_L} + i \frac{H_1(2kr_L)}{kr_L} \right), \quad (\text{B.1})$$

where J_1 is the first-class Bessel function, H_1 is the first-class Struve function and r_L is the radius of the mouth cross section.

- The second one, presented in section VI of [11], presents an expression for the acoustic radiation impedance Z_M^r of a disc in free space. This is obtained from the expressions corresponding to the real G_r and imaginary B_r parts of the acoustic radiation admittance:

$$Y_r = G_r + iB_r, \quad (\text{B.2})$$

where

$$Z_M^r = \frac{2\rho_0 c}{S_m} \frac{1}{Y_r} = \frac{2\rho_0 c}{S_m} (R^r + iX^r), \quad (\text{B.3})$$

and R^r is the resistance and X^r the reactance, real and imaginary components of the acoustic radiation impedance. As from

$$G_r = 1 + \frac{J_1(2kr_L)}{kr_L} - 2J_0(2kr_L) - \pi [J_1(2kr_L)H_0(2kr_L) - J_0(2kr_L)H_1(2kr_L)], \quad (\text{B.4})$$

$$B_r = \frac{2kr_L H_1(2kr_L)}{(kr_L - J_1(2kr_L))^2 + (H_1(2kr_L))^2}, \quad (\text{B.5})$$

we can obtain

$$R^r = \frac{G_r}{G_r^2 + B_r^2}, \quad X^r = \frac{B_r}{G_r^2 + B_r^2}. \quad (\text{B.6})$$

Acknowledgements

This work was partially supported by the Argentina National Scientific and Technical Research Council (Consejo Nacional de Investigaciones Científicas y Técnicas, CONICET) and the National University of Rosario (Universidad Nacional de Rosario, UNR). We are thankful to PhD. T. Mellow for his essential collaboration and contribution. We would also like to thank Dr. Reinaldo Welti, of whom we are modest apprentices, when studying these systems with the eyes of physicists. We are grateful to our linguistic reviewer, Sabrina María Cid Sacramone, for her suggestions on the style and correctness of our English.

Data availability statement

The data that support the findings of this study are available upon request from the authors.

References

- [1] Knight R D, Jones B and Field S 2019 *College Physics: A Strategic Approach* 4th edn (New York: Pearson).
- [2] Kinsler L E, Frey A R, Coppens A B and Sanders J V 2000 *Fundamentals of Acoustics* 4th edn (New York: Wiley).
- [3] Pearce J M 2013 *Open-Source Lab: How to Build Your Own Hardware and Reduce Research Costs*. Elsevier.
- [4] Stevenson A F 1951 *J. Appl. Phys.* **22**, 1461-1463 DOI: 10.1063/1.1699892
- [5] Campos L M B C 1984 *Journal of Sound and Vibration* **92**(2), 177-201.
- [6] Crawford F S 1967 *Waves (Berkeley Physics Course vol 3)* (New York: McGraw-Hill)
- [7] Feynman R P 1998 *The Feynman Lectures on Physics* vol 1, chapter 47 (México: Addison Wesley Longman).
- [8] Alonso M y Finn E 1970 *Física* vol 2, part 3, chapter 18, (Bogotá: Fondo Educativo Interamericano).
- [9] Gómez B J, Repetto C E, Stia C R and Welti R 2015 *Eur. J. Phys.* **36**, 55034.
- [10] Ingard U 2008 *Notes On Acoustics*. Infinity Science Press LLC, Hingham, Massachusetts. ISBN: 978-1-934015-08-7, eq. 5.53
- [11] Mellow T and Kärkkäinen L 2005 *J. Acoust. Soc. Am.* **118** (3), Pt. 1, 1311–1325.
- [12] Yang-Hann Kim 2010 *Sound propagation. An impedance based approach*. John Wiley & Sons (Asia) Pte Ltd. ISBN: 978-0-470-82583-9.
- [13] French A P 1982 *Vibrations and Waves* (New York: W W Norton and Company Inc.)